

Article

Groundwater Detection Using the Pseudo-3D Resistivity Method: A History of Case Studies

Xinjie Chen ^{1,2,3}, Zhenwei Guo ^{1,2,3} , Chunming Liu ^{1,2,3,*}, Jianxin Liu ^{1,2,3}  and Qihong Wu ^{4,*}

¹ School of Geosciences and Info-Physics, Central South University, Changsha 410083, China; chxiji@csu.edu.cn (X.C.); guozhenwei@csu.edu.cn (Z.G.); ljx6666@126.com (J.L.)

² Key Laboratory of Metallogenic Prediction of Nonferrous Metals and Geological Environment Monitoring (Central South University), Ministry of Education, Changsha 410083, China

³ Hunan Key Laboratory of Nonferrous Resources and Geological Hazard Exploration, Changsha 410083, China

⁴ School of Architecture and Civil Engineering, Chengdu University, Chengdu 610106, China

* Correspondence: liuchunming@csu.edu.cn (C.L.); wqh1016@cdu.edu.cn (Q.W.)

Abstract: With the rapid growth of the economy and population, the desire to use groundwater supplies is increasing. In order to detect groundwater, conducting a geophysics survey is a common way to map the subsurface. This method can describe the subsurface's physical properties. For example, the direct current (DC) resistivity method provides a resistivity map of the subsurface, in which the groundwater is normally located in low resistivity anomaly zones. However, the DC method needs to overcome the challenges of the urban environment, with its infrastructure and background noise. In this paper, we propose a pseudo-3D resistivity surveying method to solve these problems, and it is applied to situations of groundwater detection within the city environment, dam leakage, and drinking water. From the pseudo-3D resistivity surveying, we detected the low-resistivity anomaly in the area, which is interpreted as groundwater through borehole verification.

Keywords: pseudo-3D; resistivity; groundwater; dam leakage



Citation: Chen, X.; Guo, Z.; Liu, C.; Liu, J.; Wu, Q. Groundwater Detection Using the Pseudo-3D Resistivity Method: A History of Case Studies. *Appl. Sci.* **2022**, *12*, 6788. <https://doi.org/10.3390/app12136788>

Academic Editors: Shih-Meng Hsu, Cheng-Haw Lee and Liang-Cheng Chang

Received: 18 May 2022

Accepted: 1 July 2022

Published: 4 July 2022

Publisher's Note: MDPI stays neutral with regard to jurisdictional claims in published maps and institutional affiliations.



Copyright: © 2022 by the authors. Licensee MDPI, Basel, Switzerland. This article is an open access article distributed under the terms and conditions of the Creative Commons Attribution (CC BY) license (<https://creativecommons.org/licenses/by/4.0/>).

1. Introduction

With the rapid growth of population, urbanization, and industrialization, the sustainable utilization of water becomes more and more important. Any urbanization development is directly or indirectly related to the use of water. For any development activity, surface water and groundwater sources are the main components. The detection and exploitation of groundwater is of great practical significance to a city's populace.

However, groundwater, unlike surface water, can hardly be intuitively observed. Many zones with groundwater are associated with cracks and fractured media. Thus, groundwater exploration in hard rock terrain is a very challenging and arduous task. We have to use some special methods to detect groundwater. The geophysics method is one kind of non-destructive detection method that was widely used in recent years [1]. Some of the characteristics of this method are: easy measurement, high work efficiency, accurate detection results, and a large research area [2]. Researchers have successfully applied geophysical methods to detecting groundwater reservoirs [3]. Some examples are: electrical resistivity sounding [4], the electromagnetic method [5], and ground-penetrating radar (GPR) [6].

With the advantages of non-destructive detection, geophysical methods can be used to not only detect groundwater, but also to detect dam leakage. The most common hydrogeological problem with most dams is bedrock and lake seepage, especially fill dams built on faults and deformed structures [7]. Therefore, it is particularly important to detect and measure the dam leakage in advance to avoid the potential loss caused by the leakage of the reservoir. In order to avoid drilling or other penetrating investigations, geophysical methods with non-destructive testing are usually chosen for dam leakage detection and

monitoring. Dam leakage of groundwater is a major safety issue for dam failure. There are successful case studies published on using different methods [8], for instance, electrical methods [9–12], ground-penetrating radar (GPR) [13], seismic [14,15], and electromagnetic methods [16].

The electrical method is a useful tool for dam leakage detection and groundwater detection [17,18]. Researchers also introduced the DC resistivity method [19,20]. DC electrical resistivity imaging (ERI) is used to locate and characterize the defaults in early research [21]. Fargier employed this classical 2D ERI data acquisition system with external 3D information in the data [12]. Jodry studied the capability of the DC approach to map the dam leakage resistivity 3D distribution [22]. The research of Saad et al. is the same for groundwater exploration, which shows that groundwater will lower the resistivity value, and that silt will also decrease the resistivity value more than the effect of groundwater [17]. Due to the difference of the 3D space distribution of the embankment geometry, Nguyen and Pham studied the 3D effects on the 2D electrical resistivity tomography data inversion [23]. Alshehri and Abdelrahman conducted a 2D electrical resistivity tomography survey in the Harrat Khaybar volcanic field, northeast of Al Madinah AlMunawwarah, Saudi Arabia, to assess the presence of groundwater resources [24]. The groundwater and dam detection can both be easily achieved by 2D inline geometry. However, 3D resistivity imaging can provide more information about the groundwater and dam leakage [25].

As a traditional geophysical method, dual-frequency resistivity is widely applied in mineral exploration, groundwater exploration, and so on. Although some work on dam investigation applications and groundwater detections was carried out in the past, neither 2D nor conventional 3D electrical methods were successful in addressing the actual needs of groundwater and dam leakage detection [22]. Due to the complicated composition and the deep basement, which make it difficult to apply the conventional geophysical method, we propose a pseudo-3D resistivity method for groundwater and dam leakage detection in order to enhance the efficiency of the 3D electrical exploration. Pseudo-3D resistivity achieves similar exploration efficiency to the 2D electrical exploration with a 3D effective resistivity image. This improved approach is based on 3D DC resistivity, which is successfully applied in groundwater detection [25]. Compared to the 3D DC data array, the pseudo-3D data array provides a more efficient and effective data acquisition system.

According to the arrangement of the power supply points, the pseudo-3D resistivity method of the artificial field can be divided into branch methods, such as an inline shape, a crisscross shape, a “#” shape, and a “*” shape. In addition, based on the arrangements of the electrodes, pole–pole, pole–dipole, and dipole–dipole methods can be used. In the field of exploration geophysics, artificial field electrical exploration is divided into 1D, 2D, and 3D electrical exploration. The 1D electrical method exploration of an artificial field has a low exploration precision and a poor effect. The accuracy and effect of the 2D electrical method exploration of artificial field are better than those of 1D exploration. A pseudo-3D exploration of an artificial field is divided into the 3D electrical method exploration of measuring electrodes with a complete shape, a crisscross shape and a Γ shape [25]. Since the number of power supply electrodes and measurement electrodes are much more than those of 1D and 2D methods, it leads to a much lower efficiency than those of 1D and 2D. Therefore, although this method has a good exploration effect, it is not widely used. It is only used in some very critical exploration areas and when the funds are very sufficient.

In this paper, we utilize the pseudo-3D resistivity method, which provides higher data quality, to the Xiaojiashan Dam survey, Zixing groundwater detection survey, and the Huarong groundwater detection survey. In the investigation of the Xiaojiashan Dam, the suspected seepage location of the Xiaojiashan Dam is found through the abnormal resistivity of the inversion results. Then, the dam is checked and the corresponding reinforcement is carried out according to the seepage location. In the groundwater survey of Zixing and Huarong, based on the low resistance anomaly in the data inversion results, the geological structure near the two groundwater detection areas is judged, and the area of groundwater exploitation is divided.

2. Methods

This pseudo-3D data array provides a faster and more efficient data acquisition system than 3D data array. Additionally, the pseudo-3D data array provides more detailed information than 2D data array. The pseudo-3D resistivity method aims to find a new balance between the exploration effect and the exploration efficiency, in which the layout of the power supply points and the exploration efficiency are similar to those of the 2D resistivity method, while the arrangement of the measurement points and the exploration effect are close to the 3D resistivity method.

The pseudo-3D array uses the transmitter electrodes in a line. Figure 1 shows a schematic diagram of the field arrangement of the pseudo-3D resistivity method for different shapes. As shown in Figure 1, the “Red Crosses” are the location of the transmitter electrodes. The “Black Circles” are the location of the receiver electrodes. As shown in Figure 1a,b, from A₋₁₃ to A₁₃, the distance is 2.6 times the width of square 6. The infinitely powered electrode is located at position 1. The transmitter equipment is located at position 3. We assume that the coordinates (−a, −b) and (a, b) are at the corners of square 6. The coordinates of the transmitter electrodes (x, y) are given as:

$$(x, y) = \begin{cases} (x, 0); & \text{when } |x| \leq a \\ (a + 2^i, 0); & \text{when } a < x \leq (3a + 1) \\ (-a - 2^i, 0); & \text{when } -(3a + 1) \leq x < -a \end{cases} \quad (1)$$

where x, y, a, i are integers.

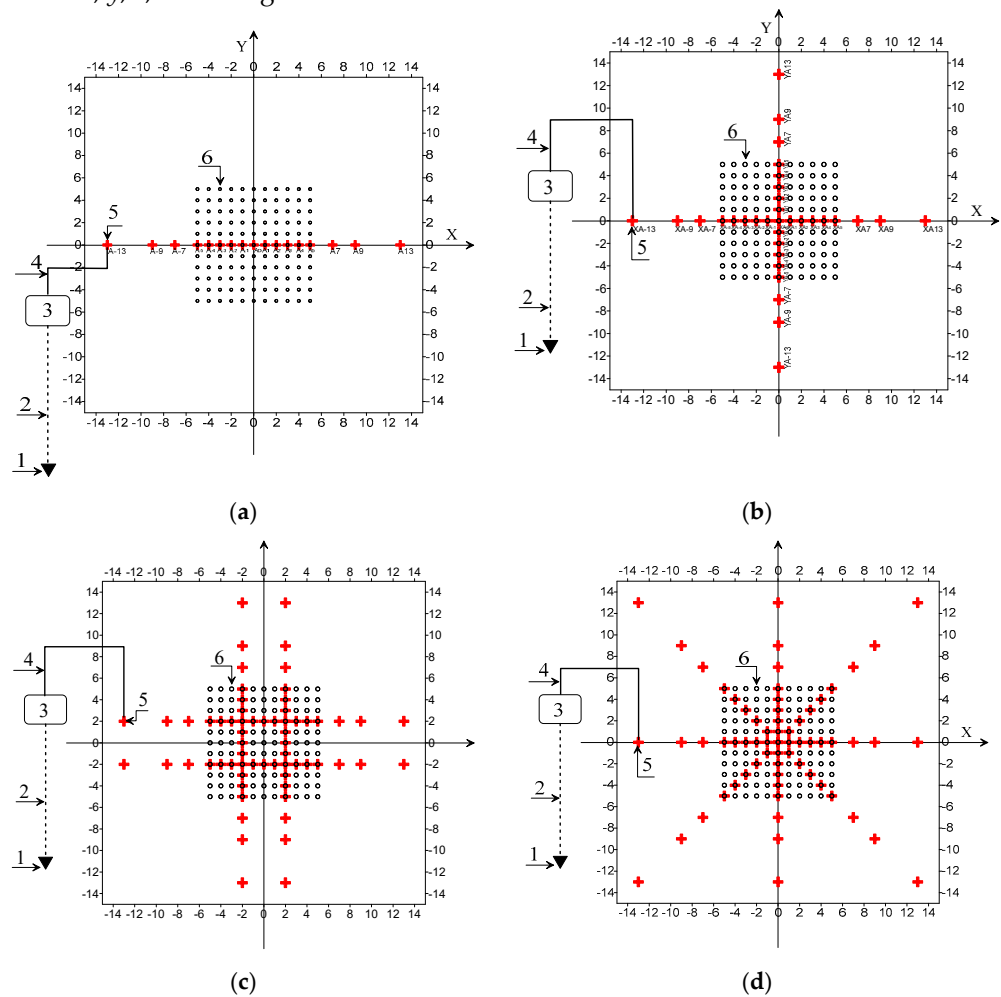


Figure 1. The observation system of pseudo-3D resistivity surveying, (a) inline shape, (b) crisscross shape, (c) “#” shape, and (d) “*” shape.

The neighbor distance is c in the horizontal direction (X); and d in the vertical direction (Y). When the distance of the transmitter line is 2.6 times the width of square 6, the coordinate origin is assumed to be the center of the measurement area.

The coordinates of the transmitter are given as:

$$(X_c, Y_c) = (x \times c, y \times d) = (x \times c, 0) \quad (2)$$

The pseudo-3D array can measure the data using the pole–pole and pole–dipole methods.

We mainly apply the inline pseudo-3D resistivity method to groundwater detection and dam leakage detection. Based on the characteristics of the exploration targets and topography, the pseudo-3D resistivity method uses the transmitters to power the underground through the electrodes, then, the receivers simultaneously receive the electric field signals from all the measurement locations. The receivers obtain the apparent resistivity and the induced electric parameters when each power supply point of the corresponding shape is obtained, which completes the exploration.

3. Case Studies

In this section, we apply pseudo–3D resistivity to remove the groundwater problems in three cases. The pseudo–3D resistivity method of the inline shape is used, as shown in Figure 1a. It uses a dipole–pole multi-point source electric method exploration device, which belongs to a multi-power frequency division and simultaneous power supply device.

3.1. Dam Leakage Detection

The Xiaojiashan Reservoir survey area is located in the northeastern part of Hunan Province, as shown in Figure 2. It is a medium-sized water conservancy project with comprehensive utilization benefits, such as water supply and flood control. The results of the previous investigation indicate that the dam has potential safety hazards, and that the cause of seepage should be detected and controlled to maintain the integrity and safety of the dam. Due to its location in a karst area, the geological conditions of the Xiaojiashan Reservoir are complex. The structural karsts and fractures are developed, and the dam seepage is serious.

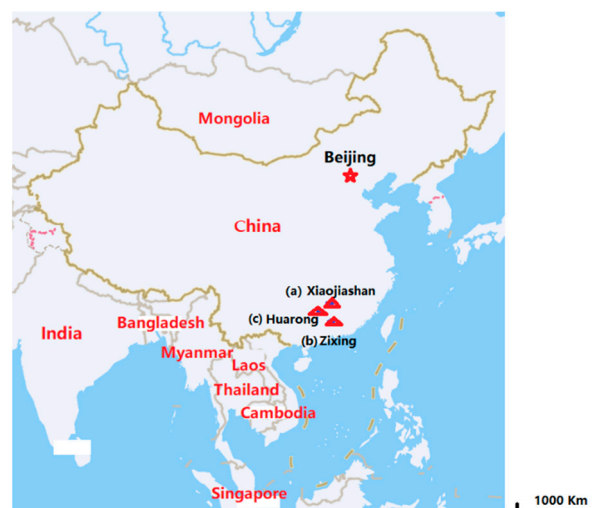


Figure 2. Geographic location map of surveys, (a) Xiaojiashan Reservoir leakage survey, (b) Zixing groundwater detection survey, (c) Huarong groundwater detection survey.

Since the numerical modeling results were published [25], here, we directly apply the method to the dam leakage detection. The Xiaojiashan Dam (Figure 3) presents a risk of leakage, so it is necessary to perform a detection. The pseudo-3D resistivity array

is designed as shown in Figure 3. We select the inline pole–dipole device artificial field pseudo–3D resistivity method in this experiment. The 61 green dots indicate the locations of transmitter electrodes. The 90 purple dots indicate the locations of receiver electrodes. The red rectangle is the investigation area. The distances between the successive receiver electrodes are 10 m. In total, we have acquired 3280 pseudo–3D resistivity datasets.



Figure 3. Pseudo-3D arrays for Xiaojiashan Dam leakage detection.

The pseudo-3D inversion results of the resistivity data are shown in Figure 4a. The results can be described by a 3D resistivity cube. Based on the pseudo-3D electric field experimental results of the Xiaojiashan Reservoir and the cube, we can infer the location of the leakage. Because of the low resistivity, the leak path may show a conductive anomaly in the cube. The channel of the dam is suspected to be the shallow part of the dam, which is marked by a blue arrow. The green part is the low resistivity anomaly, which is separated in Figure 4b.

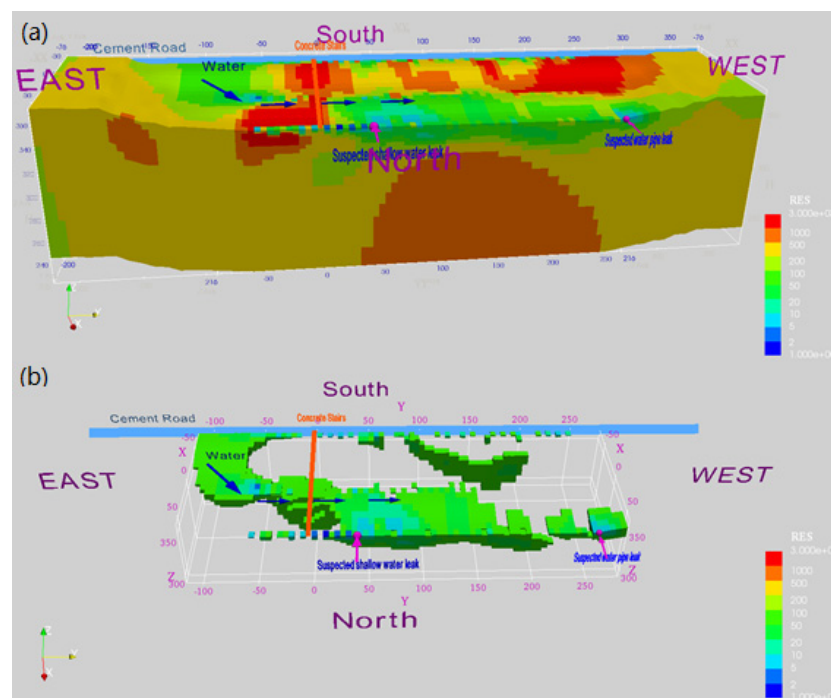


Figure 4. Pseudo–3D resistivity data inversion results. (a) resistivity cube, (b) low resistivity path.

We infer that the dam has a weak layer in the obvious elevation of the current path, and the weak layer does not exhibit a low-resistivity anomaly in the corresponding elevation of profile 1. It is suspected that the pre-stage grouting treatment has strengthened some weak layers. It is recommended to collect some data for the specific parts that went through the previous grouting treatment.

Figure 5 illustrates the resistivity image by profile (a) 1, (b) 2, and profile (c) 3. Based on the experimental results stereoscopic, the $-120\sim-40$ th measurement location in profile 1 and the $-100\sim-40$ th measurement location in profile 2 exhibit low resistivity. The anomaly zone is approximately vertical to the dam direction. Figure 5b shows that a low-resistivity anomaly converges within the vicinity of the 0th measurement point in profile 2. The low-resistivity anomaly starts to become shallower near the 10th measurement point of profile 2. Then, this low-resistivity anomaly zone, paralleled with reservoir dam formation, is suspected to be the dam seepage.

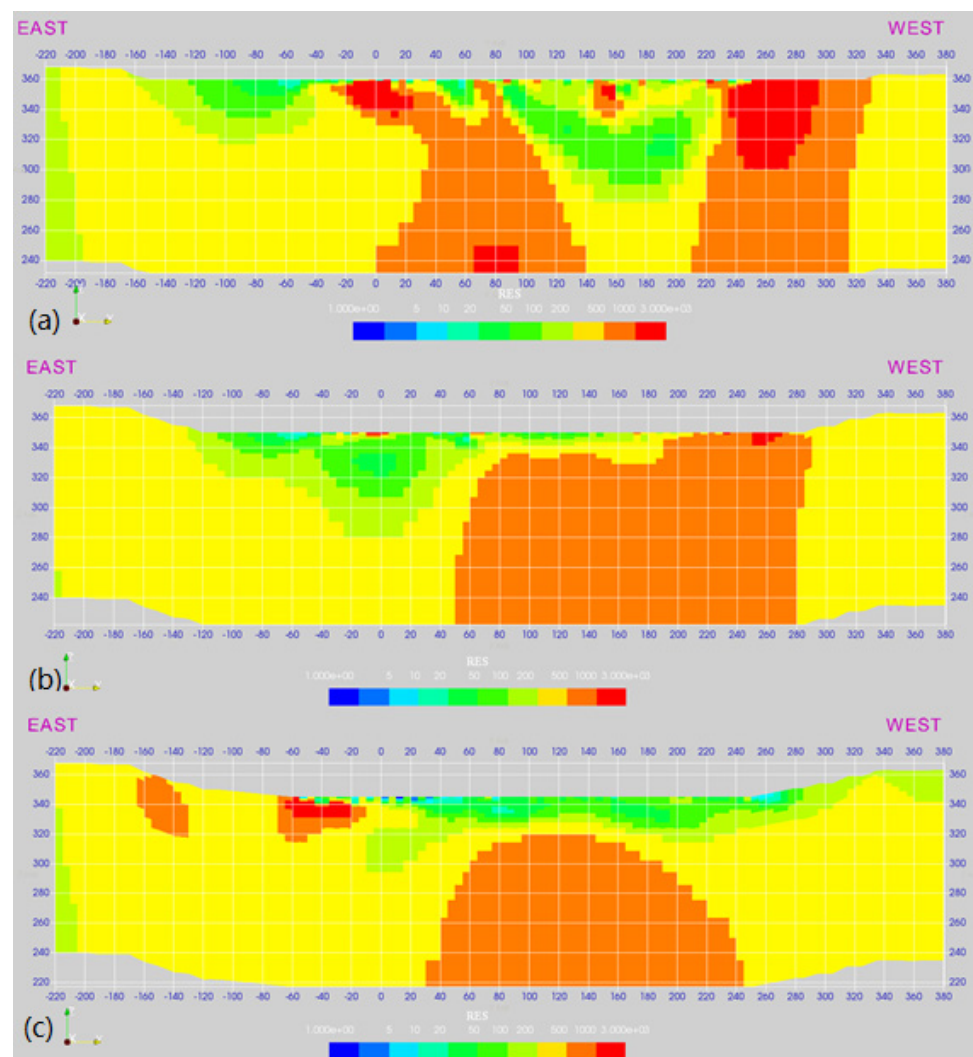


Figure 5. Sectional view of pseudo-3D resistivity inversion results of (a) profile 1, (b) profile 2, and (c) profile 3 in the Xiaojiashan Reservoir.

In Figure 5a, a low resistivity anomaly zone is detected between the location -40 and the 220 measurement location. It is also detected on profile 2 (Figure 5b). We infer that the low resistivity anomaly is mainly located in the measurement points segment of profile 1.

In Figure 5b, the shallow part of the –110~160th measurement location of profile 2 shows a low resistivity anomaly trend, where the center of the low resistivity anomaly zone is located near the 0-station. The depth of the low resistivity anomaly is around 40 m.

In Figure 5c, the shallow surface of the 0~270 measurement locations shows a low resistivity zone. At the 40th measurement location, an obvious low-resistivity anomaly reaction is presented. The obvious seepage near the 40th measurement point of profile 2 (Figure 5b) has a long-term influence on the surrounding soil of profile 3 (Figure 5c). An obvious low-resistivity anomaly near the 260th measurement location in profile 3 is inferred as the leakage of the ground water pipe.

Based on the stereoscopic and sectional view of the artificial field pseudo-3D resistivity method experimental results in the Xiaojiashan Reservoir, the dam leakage is inferred as the 1st-1~120th measurement locations →, the shallow part of the –00~–40th measurement section of profile 2 →, the vicinity of the –40~20th measurement location of profile 2 →, the 2nd-20~160th measurement locations →, and the 0~240th measurement location of profile 3 (Figure 5c).

Based on the resistivity image in Figure 5, the continuous low resistivity indicates that the leakage is parallel to the dam's direction. The seepage is inferred to flow from the east of the dam, where the reservoir water seeps through the weak layer in the dam. However, profile 1 is 30 m away from the reservoir water, so the low resistivity anomaly may also be from the east side of the dam.

It is observed that the surface of the reservoir water is lower than the leakage and that the anomaly of the 120~–40th measurement locations in profile 1 follow the vertical direction of the dam, which can be inferred as the channel of the reservoir water. Based on these observations, the leakage water is suspected to come from reservoir water and underground water near the mountain on the east side of the dam.

3.2. Groundwater Exploration Cases

3.2.1. Groundwater Survey in Zixing City with Geophysical Methods

The Zixing groundwater detection survey area is located in the northeastern part of Zixing City, the southern part of Hunan Province, the intersection of Hunan, Guangdong and Jiangxi provinces, and the Dongjiang Lake Scenic Area (Figure 2). According to previous geological surveys, the exposed strata in the study area is the Middle Devonian Tiaomajian Formation (D2t), which is distributed in the southwest corner of the work area, and belongs to the sediment and clastic deposits of continental facies transitioning to coastal facies. The lithology is a gray-white medium-fine-grained quartz sandstone and a gravel-bearing quartz sandstone. The main outcrop in the working area is a compressive fault, which runs through the entire working area and goes north to northeast. Near the fault zone, silicification and alteration are serious, and the zone is locally altered into quartzite. According to regional information, the layer thickness is 78–300 m.

The combined profiling method, resistivity sounding method, and CSAMT are limited by geology and other factors, and the exploration effect is poor. The pseudo-3D resistivity method is added to identify the distribution of relevant faults in the survey areas of Hejiashan and Zhoumensi. Among them, the HJS-03 survey line of Hejiashan is selected to compare the results of the pseudo-3D resistivity method and those of the resistivity sounding method (in Figure 6).

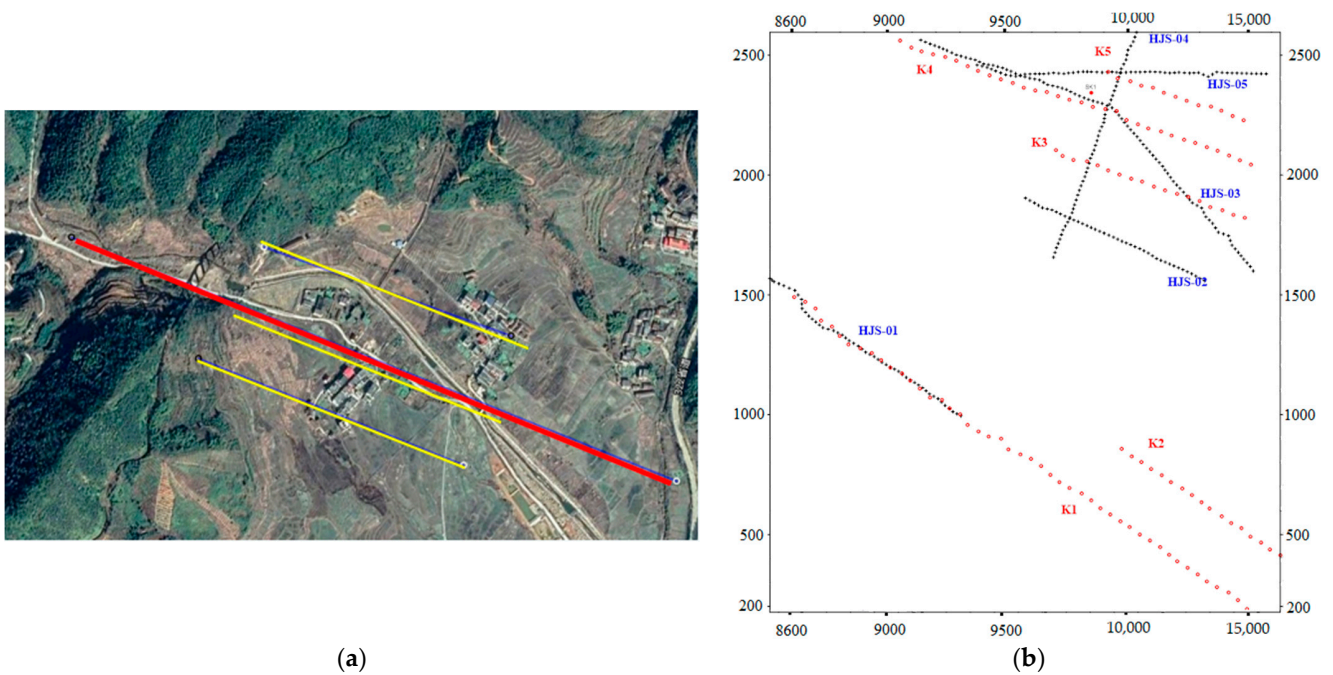


Figure 6. Geophysical prospecting arrays in Hejiashan survey area. (a) Pseudo-3D arrays. (b) The combined profiling method, resistivity sounding method, and CSAMT arrays (the black cross-shaped measuring points are the combined profiling and resistivity sounding points, and the red circles are the CSAMT measuring points).

In Figure 7, there is a low-resistance anomaly tilting towards the large measuring point between No. 250–400 measuring points, and the dip angle is about 50 degrees. It is speculated that the low-resistivity anomaly and the F1 fault have caused rock fragmentation, water content increase, and NW trend factors, such as the presence of rivers. It is speculated that the low-resistance anomalies with an elevation of less than 300 m between the measuring points 560–850 are the combined reaction of Quaternary alluvial layers, streams, NW-trending rivers, and fractured zones. From the perspective of water exploration, due to the presence of the NNE-trending F1 fault and the NW-trending fracture zone near the HJS-03 line, it is speculated that the surrounding area of this survey line is a favorable area for water exploration. As a result, follow-up data analysis should be carried out in combination with other results to verify the speculation.

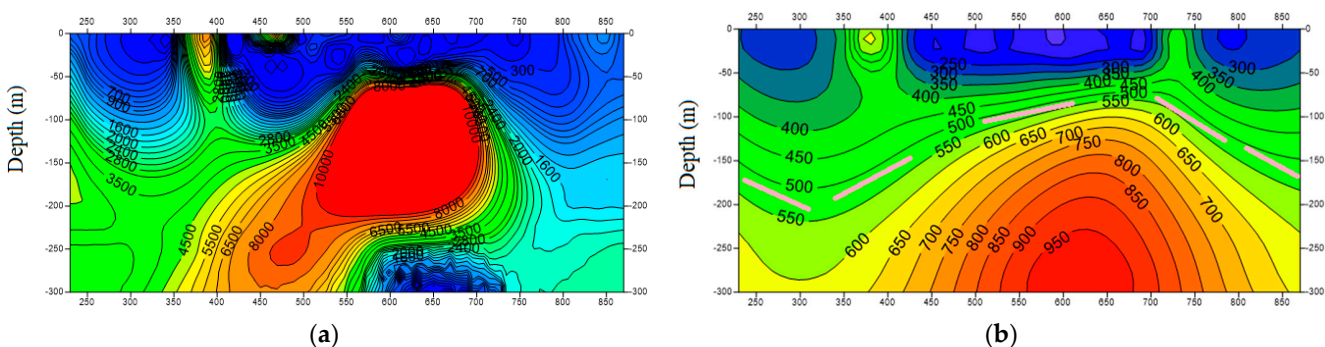


Figure 7. The resistivity sounding and pseudo-3D resistivity inversion results of the HJS-03 survey profile. (a) Resistivity sounding result. (b) Pseudo-3D resistivity result (the red lines represent fault and the pink lines segment layer the resistivity).

Combined with the geophysical prospecting in the Zixing groundwater survey, it is found that the F1 fault has a relatively obvious display in the survey area. The inclination angle is about 50~70 degrees. The F1 fault has an obvious abnormal response in profile

HJS-03 and profile HJS-05 in the Hejiashan survey area, and the F1 fault has a relatively obvious abnormal response in profile ZMS-01 in the Zhoumensi survey area. In addition, near the No. 2100 measuring point of profile K1 and the No. 350 measuring point of profile K2 in the Hejiashan survey area, it is speculated that there is a fault with better water content. Profile K4 is mainly located in the river valley, and it is speculated that there are structures in multiple directions. Therefore, the results of this exploration line need to be focused on the superposition effect of structures in multiple directions. The water content between the No. 700~1400 measuring points is relatively strong, and there are relatively complete granites. From the perspective of the deep aquifers, it satisfies the conditions needed to form hot water. There is a fault with good water content near the No. 400 measuring point of profile K8 and the No. 350 measuring point of profile K9 in the Zhoumensi survey area.

3.2.2. Groundwater Survey in Huarong County with Geophysical Methods

The Huarong groundwater survey is located in the seat of the government of Huarong County. Huarong County is a county in the west of Yueyang City, Hunan Province, located in the north of Dongting Lake (Figure 2). The survey area boundary is mainly composed of rivers and lakes accumulation plain landforms, and most of the landforms are flat except for local ridges and hills. The topography is high in the northwest and low in the southeast. The previous geological survey shows that the exposed strata in the Huarong mineral water plant are simple, mainly the Baishajing Formation of Middle Pleistocene of the Quaternary and the first to fifth members of the Lengjiaxi Group of the Pre-Sinian.

We have carried out the combined profiling method, resistivity sounding method, CSAMT and pseudo-3D resistivity method on the Huarong survey (in Figure 8). Since the fault development depth in this area is not large, the stratum electrical properties are not very different, and the 2D resistivity sounding exploration response ability is limited. As a result, there will be a certain degree of error in judging the position of the stratigraphic contact surface. Therefore, the pseudo-3D resistivity method is added for exploration, and it is the main basis for later drilling. A total of six survey profiles were completed in this pseudo-3D resistivity array, named as profiles L1, L2, L3, L4, L5, and L6.

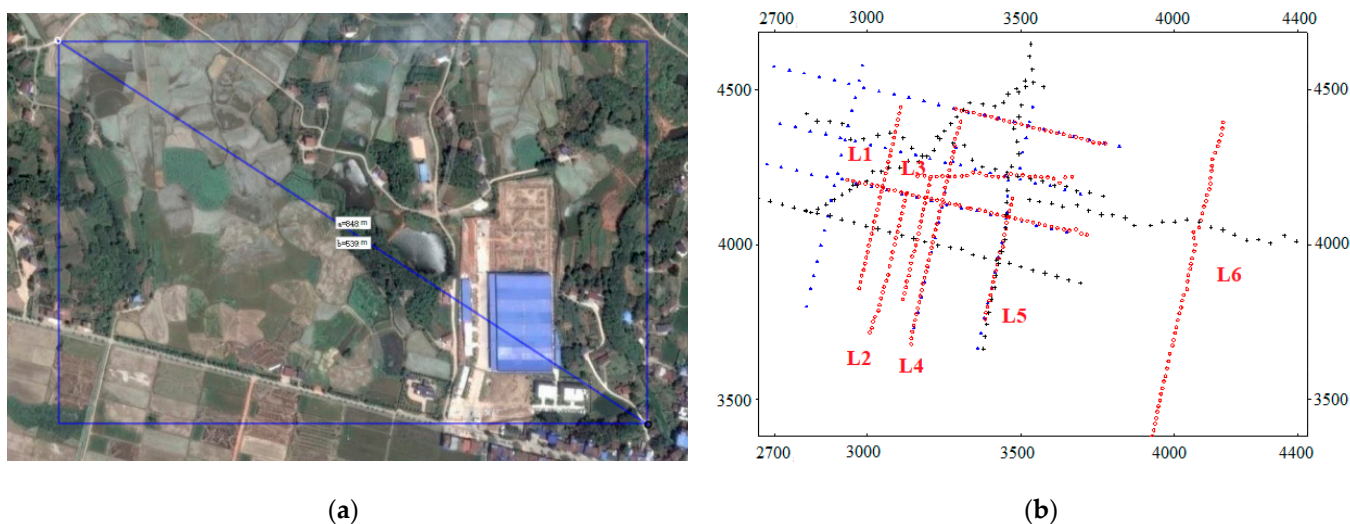


Figure 8. Geophysical prospecting arrays in the Huarong Survey Area. (a) Pseudo-3D arrays. (b) The combined profiling method, resistivity sounding method, and CSAMT arrays (the black cross-shaped measuring points are the combined profiling and resistivity sounding points, and the red circles are the CSAMT measuring points. The black cross-shaped measuring points are the pseudo-3D resistivity point).

The profile L1 is 570 m long. The distance between two consecutive points is 30 m. The total number of measuring points is 19, and the azimuth angle is 57 degrees.

In Figure 9, it is speculated that there is a NW-trending fault passing near the No. 255 measuring point. The electrical sounding results at this location obviously show an abnormal response of shallow low resistance, and that the resistivity increases significantly to 400 Ω m at a depth of about 100 m. Therefore, it is speculated that there is a good water-conducting fracture in this part, and that there is a contact surface between the muddy and sandy strata, so it is speculated that there should be a good aquifer there.

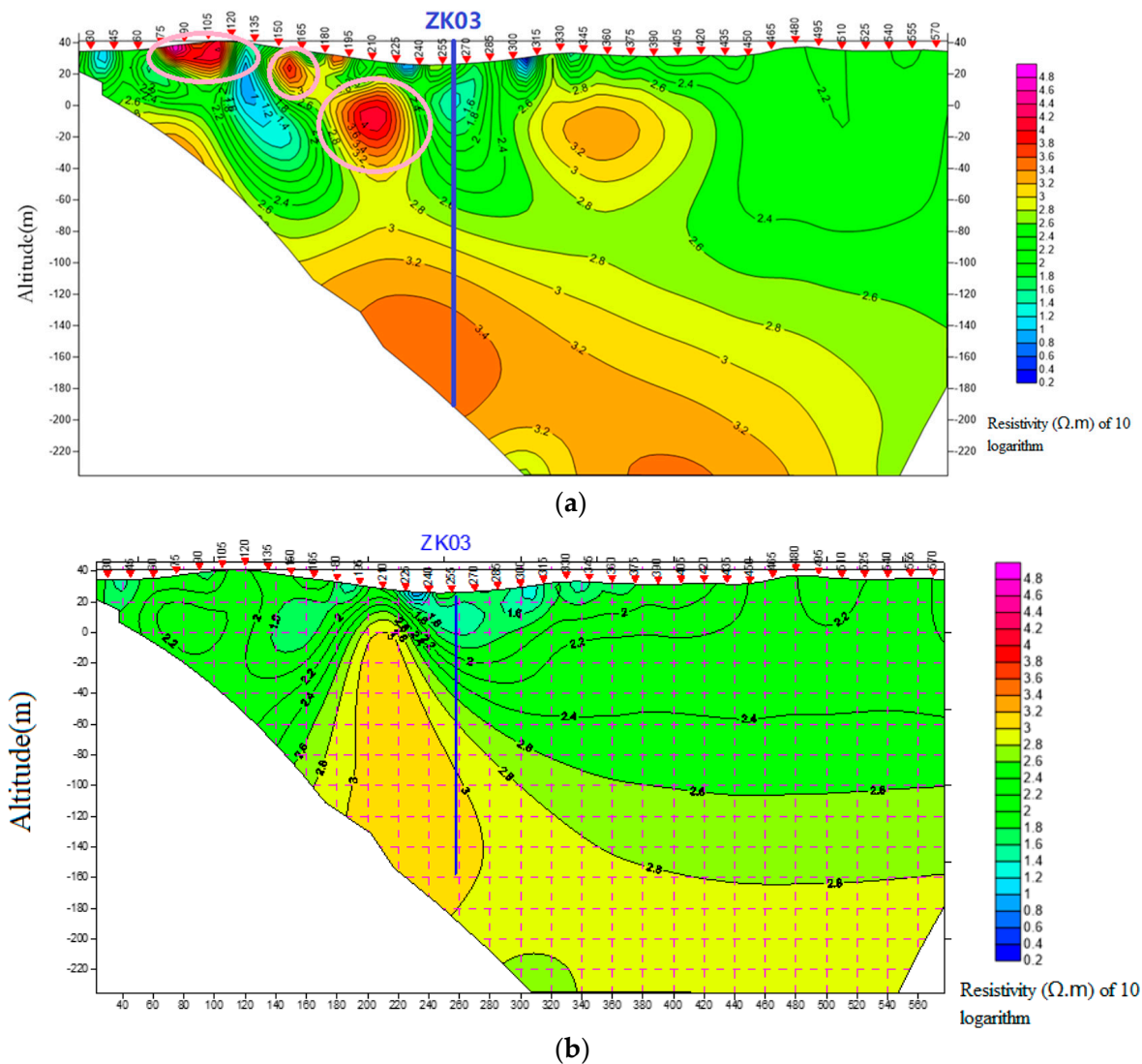


Figure 9. The resistivity sounding and pseudo–3D resistivity inversion results of L1 survey profile. (a) Resistivity sounding result. (b) Pseudo–3D resistivity result (the value of the median line in the figure is the base 10 logarithm of the resistivity). The blue lines indicate the locations of boreholes.

In the later period, the No. ZK03 verification hole is arranged near the No. 255 measuring point. The verification results show that the slate with high argillaceous composition is mainly at a depth shallower than 100 m, and that the sandy composition was increased below 100 m, which is an obvious shale at the contact surface. Fractures develop in the sandy stratum below the contact surface. Judging from the water output, the water exposed by the hole is mainly confined water, and the water tends to flow out from the surface of the borehole pipe. The later pumping test shows that the water output of this hole is about 410 tons, which is very high, and that the verification results are in good agreement with the inferred results.

The profile L2 is 640 m long. The distance between consecutive points are 40 m. The total number of measuring points is 16, and the azimuth angle is 105 degrees.

In Figure 10, between No. 160 and No. 240 of profile L2, it is speculated that the F2 fault passes through. The pseudo-3D resistivity results show that there is an obvious “V”-shaped low-resistivity anomaly here, and that the low-resistivity anomaly is thicker than 200 m. It is speculated that the low resistivity anomaly in the range of this measuring point is mainly the reaction of argillaceous slate. Since there is a resistivity interface in this measuring point, it is speculated that it is the contact surface of argillaceous slate and quartz sandstone formation, and that there are water-bearing fractures in this contact surface.

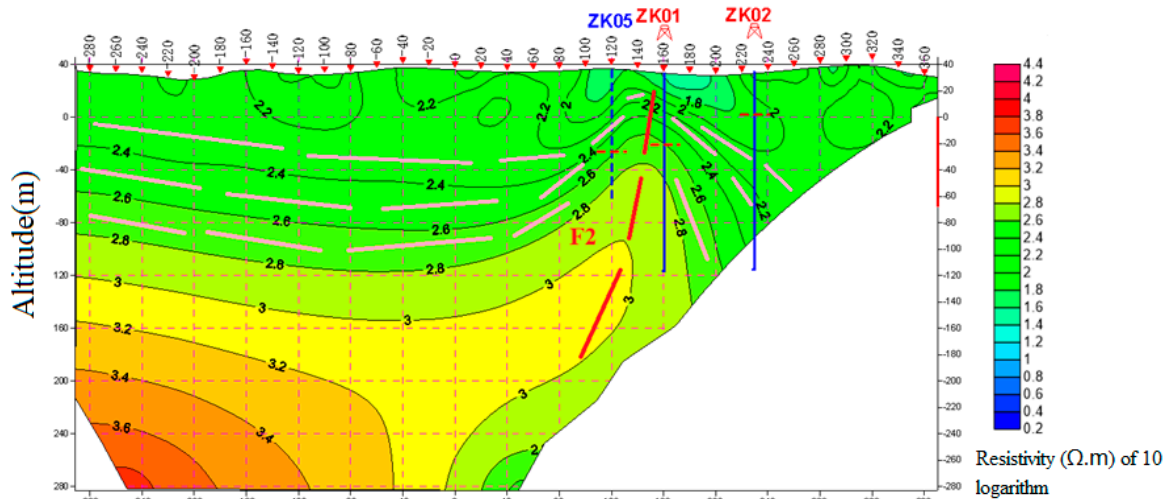


Figure 10. The pseudo-3D resistivity inversion results of the L2 survey line. The value of the median line in the figure is the base 10 logarithm of the resistivity (the red lines represent the fault. The pink lines in the segment layer represent the resistivity. The blue lines indicate the locations of boreholes).

In the later stage, ZK05, ZK01, and ZK02 verification holes are arranged near measuring points No. 120, 160, and 220, respectively (in Figure 11). The verification results show that the slate with high argillaceous content is mainly at the depth of 80 m. Also, when the slate is below 80 m, the sandy composition increases. There is an obvious crushing phenomenon at the contact surface, and the sandy stratum below the contact surface develops fractures. The later pumping test shows that the maximum water output of ZK01 is about 460 tons, that of ZK02 is about 170 tons, and that of ZK05 is about 100 tons. It is speculated that the change in water output is due to the F2 fault.

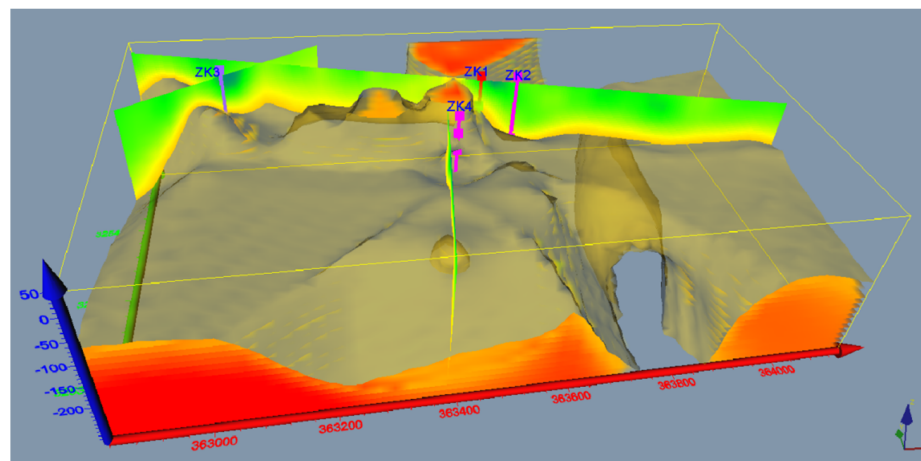


Figure 11. Pseudo-3D resistivity in Huarong County, Nanshan Township.

After the combined profiling method, resistivity sounding method, CSAMT, and the pseudo-3D resistivity method are carried out in the Huarong groundwater survey, it is found that there are relatively obvious fault indications in the survey area. Also, there are two structural damage areas, which are presumed to result from the intersection of the different directional faults, causing rock fragmentation, increased water content, and reduced resistivity.

In the macroscopic parts where faults or broken zones pass through, the pseudo-3D resistivity results show that there is a steeper resistivity contact surface, which is presumed to be between argillaceous slate and sandy slate, and that fractures are often found on this contact surface. This provides a good condition for the collection of water and a good guide for the selection of verification holes. The resistivity value of the two lithological contact surfaces reflected by the electrical sounding results is about 400 Ω m. The parameters are used to judge the position of the contact surface, and the contact surface can often form a relatively obvious broken layer. The best practice is to try to avoid areas where the resistivity is significantly lower or higher and the thickness is larger.

4. Discussion

ERM is proven to be the most effective technique in mapping groundwater resources, as the groundwater resource is largely localized and difficult to be mapped [26]. Thus, this technique is of great importance in providing the initial result of groundwater detection. However, the hydrological interpretation of geoelectric results can be very ambiguous due to the extremely wide resistivity ranges which characterize both freshwater bearing aquifers as well as overlying and underlying strata [3].

In electrical resistivity surveys, high resolution and reliable imaging depends on the choices of electrode configuration, which is normally known as an array [27]. We have presented a pseudo-3D resistivity method which uses a dipole–pole multi-point source electric method exploration device. Notice that the survey line should be placed perpendicular to the strike of the targeted structure, which overcomes the limitation of the 2-D survey method [28].

In the case of groundwater geophysical surveys in Zixing, according to profiles K8 and K9, the resistivity image from the pseudo-3D resistivity detection (in Figure 7b) provided a nice subsurface resistivity distribution map with clear anomalies. In the study of Alshehri and Abdelrahman, the high resistivity anomaly was located in a shallow part, but it was not explained very well [24]. According to the data, we speculated that there is a northwest-trending fault nearby, dipping southwest at an angle of about 50 degrees.

Another groundwater geophysical survey in Huarong provided a similar successful case study. In this survey, the 2D DC resistivity inversion results indicate that the layers were discrete (i.e., the high resistivity anomalies were not connected in Figure 9a) because it could not clearly divide layers in deep areas due to the inhomogeneous properties of the soil material [26]. The faults and broken zones were filled up with groundwater and are characterized as low resistivities in the pseudo-3D resistivity survey (in Figure 9b). Because the groundwater reservoirs are typically found in saturated sand, saturated sandy clay, and saturated silt, clay, and sand [17], there was a steeper resistivity contact surface, which was between argillaceous slate and sandy slate. The resistivity values of the two lithological contact surfaces were about 400 Ω .m. It was used to infer the position of the contact surface. Compared with the drilling results, the resistivity interpretations had high authenticity.

The groundwater reservoir was normally related with the faults or broken zones [7]. When it came to the Xiaojiashan Dam leakage surveys, we inferred a low-resistivity anomaly between the station of the –120~–40th measurement location in profile 1 to be the location of seepage. Moreover, we inferred that the water source comes from a mountain crevice on the east side of the dam by using pseudo-3D resistivity inversion. The second channel of the dam leakage path, clear from the inversion result, is characterized by an obvious low-resistivity anomaly in the superficial view of the 0~40 measurement location in profiles 2 and 3. The water came from the east side of the dam, and the groundwater seeps into

the dam through the fissures and flows through the weak layer of the dam. The source of seepage was related to the reservoir and the groundwater of the mountain on the east side of the dam.

The pseudo-3D method has a better resistivity exploration effect than the 2D resistivity method due to better resolution. However, we note that the limitation of the pseudo-3D resistivity is the high computational cost compared with the 2D resistivity method.

5. Conclusions

Based on all the case studies presented, the pseudo-3D resistivity method has successfully helped researchers find out the distribution of relevant faults around the groundwater surveys, and provided relevant information for subsequent water exploration work. The groundwater was clearly detected with support from the borehole data as this technique has efficient exploration and flexibility.

In order to combine the 2D resistivity method with the pseudo-3D resistivity method in groundwater exploration, the 2D resistivity method needs to be first carried out, and then the 2D resistivity method is applied to the key areas. In special terrain areas where it is difficult to carry out the 2D resistivity method or the 3D, the pseudo-3D resistivity method can be directly used.

Author Contributions: Conceptualization, Z.G. and X.C.; methodology, X.C.; software, C.L.; validation, Z.G., C.L. and J.L.; formal analysis, Z.G. and C.L.; investigation, C.L.; data curation, C.L. and Q.W.; writing—original draft preparation, Z.G. and X.C.; writing—review and editing, Z.G., C.L. and X.C.; visualization, J.L.; supervision, J.L.; funding acquisition, C.L. and Q.W. All authors have read and agreed to the published version of the manuscript.

Funding: This research is supported by the Natural Science Foundation of China (NSFC) [42074169], Innovation-Driven Youth Team Project of Central South University [2020CX0012], Hunan Province Natural Resources Science and Technology Project “Key Technologies and Applications of Polluted Site Detection and Evaluation in Urban Physical Examination” No.: 2022-25 and Regional Innovation Cooperation Programs of Sichuan province (2021YFQ0050).

Conflicts of Interest: The authors declare no conflict of interest.

References

1. VenkataRao, G.; Kalpana, P.; Rao, R.S. Groundwater investigation using geophysical methods—A case study of Pydibhimavaram Industrial area. *Int. J. Res. Eng. Technol.* **2014**, *3*, 13–17.
2. Pereira, P.A.; Lima OA, L. Estrutura elétrica da contaminação hídrica provocada por fluidos provenientes dos depósitos de lixo urbano e de um curtume no município de Alagoinhas, Bahia. *Rev. Bras. Geofis.* **2007**, *25*, 5–19. [[CrossRef](#)]
3. Goldman, M.; Neubauer, F.M. Groundwater exploration using integrated geophysical techniques. *Surv. Geophys.* **1994**, *15*, 331–361. [[CrossRef](#)]
4. Amaruddin, H.I.; Hassan, R.; Mohd Amin, N.; Abd Malek, N.J. Finite Element Model of Mortise and Tenon Joint Fastened with Wood Dowel Using Kempas Species. In *CIEC 2013*; Springer: Singapore, 2014; pp. 3–14.
5. Siemon, B.; Christiansen, A.V.; Auken, E. A review of helicopter-borne electromagnetic methods for groundwater exploration. *Near Surf. Geophys.* **2009**, *7*, 629–646. [[CrossRef](#)]
6. Maheswari, K.; Senthil Kumar, P.; Mysaiah, D.; Ratnamala, K.; Sri Hari Rao, M.; Seshunarayana, T. Ground penetrating radar for groundwater exploration in granitic terrains: A case study from Hyderabad. *J. Geol. Soc. India* **2013**, *81*, 781–790. [[CrossRef](#)]
7. Al-Fares, W. Contribution of the geophysical methods in characterizing the water leakage in Afamia B dam, Syria. *J. Appl. Geophys.* **2011**, *75*, 464–471. [[CrossRef](#)]
8. Karastathis, V.K.; Karmis, P.N.; Drakatos, G.; Stavrakakis, G. Geophysical methods contributing to the testing of concrete dams, application at the Marathon Dam. *J. Appl. Geophys.* **2002**, *50*, 247–260. [[CrossRef](#)]
9. Abu-Zeid, N. Investigation of channel seepage areas at the existing Kaffrein Dam Site (Jordan) using electrical resistivity measurements. *J. Appl. Geophys.* **1994**, *32*, 163–175. [[CrossRef](#)]
10. Aina, A.; Olorunfemi, M.O.; Ojo, J.S. An integration of aeromagnetic and electrical resistivity methods in dam site investigation. *Geophysics* **1996**, *61*, 349–356. [[CrossRef](#)]
11. Cho, I.K.; Yeom, J.Y. Crossline resistivity tomography for the delineation of anomalous seepage pathways in an embankment dam. *Geophysics* **2007**, *72*, G31–G38. [[CrossRef](#)]
12. Fargier, Y.; Lopes, S.P.; Fauchard, C.; François, D.; Côte, P. DC-electrical resistivity imaging for embankment dike investigation: A 3D extended normalisation approach. *J. Appl. Geophys.* **2014**, *103*, 245–256. [[CrossRef](#)]

13. Xu, X.X.; Zeng, Q.S.; Li, D.; Wu, J.; Wu, X.G.; Shen, J.Y. GPR detection of several common subsurface voids inside dikes and dams. *Eng. Geol.* **2010**, *111*, 31–42. [[CrossRef](#)]
14. Karastathis, V.K.; Karmis, P.N.; Drakatos, G.; Stavrakakis, G. Assessment of the dynamic properties of highly saturated concrete using one-sided acoustic tomography. Application in the Marathon Dam. *Constr. Build. Mater.* **2002**, *16*, 261–269. [[CrossRef](#)]
15. Samyn, K.; Mathieu, F.; Bitri, A.; Nachbaur, A.; Closset, L. Integrated geophysical approach in assessing karst presence and sinkhole susceptibility along flood-protection dykes of the Loire River, Orléans, France. *Eng. Geol.* **2014**, *183*, 170–184. [[CrossRef](#)]
16. Berga, L.; Buil, J.M.; Bofill, E.; De Cea, J.C.; Perez, J.G.; Mañueco, G.; Yagüe, J. Dams and Reservoirs, Societies and Environment in the 21st Century, Two Volume Set. In Proceedings of the International Symposium on Dams in the Societies of the 21st Century, 22nd International Congress on Large Dams (ICOLD), Barcelona, Spain, 18–23 June 2006.
17. Saad, R.; Nawawi MN, M.; Mohamad, E.T. Groundwater detection in alluvium using 2-D electrical resistivity tomography (ERT). *Electron. J. Geotech. Eng.* **2012**, *17*, 369–376.
18. Michalis, P.; Sentenac, P.; Macbrayne, D. Geophysical assessment of dam infrastructure: The mugdock reservoir dam case study. In Proceedings of the 3rd Joint International Symposium on Deformation Monitoring (JISDM), Vienna, Austria, 30 March–1 April 2016.
19. Keller, G.V. DC resistivity methods for determining resistivity in the earth's crust. *Phys. Earth Planet. Inter.* **1975**, *10*, 201–208. [[CrossRef](#)]
20. Sumner, J.S. *Principles of Induced Polarization for Geophysical Exploration*; Elsevier: Amsterdam, The Netherlands, 1976; p. 277, ISBN 0-444-41481-9.
21. Palma-Lopes, S.; Fauchard, C.; Mériaux, P.; Auriau, L. Rapid and cost-effective dike condition assessment methods: Geophysics. *Geography* **2012**, *32*, 1–17.
22. Jodry, C.; Lopes, S.P.; Fargier, Y.; Cote, P.; Sanchez, M. A cost-effective 3D electrical resistivity imaging approach applied to dike investigation. *Near Surf. Geophys.* **2017**, *15*, 27–41. [[CrossRef](#)]
23. Nguyen, T.N.; Pham, K.N. Correcting the distortion of apparent resistivity pseudosection produced by 3D effect of the embankment geometry. *Environ. Earth Sci.* **2018**, *77*, 105. [[CrossRef](#)]
24. Alshehri, F.; Abdelrahman, K. Groundwater resources exploration of Harrat Khaybar area, northwest Saudi Arabia, using electrical resistivity tomography. *J. King Saud Univ.-Sci.* **2021**, *33*, 101468. [[CrossRef](#)]
25. Guo, Z.; Liu, C.M.; Liu, J.X.; Zhou, H.; Zhao, S.J.; Li, H.B. Pseudo-3D direct current resistivity for underground water surveying. In Proceedings of the 24th EM Induction Workshop, Helsingør, Denmark, 12–19 August 2018; Available online: https://emiw2018.emiw.org/fileadmin/emiw2018/abstracts/3.0_pseudo-3d_direct-current_guo.pdf (accessed on 12 August 2018).
26. Riwayat, A.I.; Nazri MA, A.; Abidin MH, Z. Application of electrical resistivity method (ERM) in groundwater exploration. In *Journal of Physics: Conference Series*; IOP Publishing: Batu Pahat, Malaysia, 2018; Volume 995, p. 012094.
27. Aizebeokhai, A.P. 2D and 3D geoelectrical resistivity imaging: Theory and field design. *Sci. Res. Essays* **2010**, *5*, 3592–3605.
28. Rolia, E.; Sutjiningsih, D. Application of geoelectric method for groundwater exploration from surface (A literature study). In *AIP Conference Proceedings*; AIP Publishing LLC: Melville, NY, USA, 2018; Volume 1977, p. 020018.